This article has been accepted for publication in a future issue of this journal, but has not been fully edited. Content may change prior to final publication. Citation information: DOI 10.1109/JSTSP.2015.2467355, IEEE Journal of Selected Topics in Signal Processing

Moving Target Detection in Distributed MIMO Radar on Moving Platforms

Hongbin Li, *Senior Member, IEEE*, Zhe Wang, *Student Member, IEEE*, Jun liu, *Member, IEEE* and Braham Himed, *Fellow, IEEE*

***Abstract*—This paper examines moving target detection in distributed multi-input multi-output radar with sensors placed on moving platforms. Unlike previous works which were focused on stationary platforms, we consider explicitly the effects of platform motion, which exacerbate the location-induced clutter non-homogeneity inherent in such systems and thus make the problem significantly more challenging. Two new detectors are proposed. The first is a sparsity based detector which, by exploiting a sparse representation of the clutter in the Doppler domain, adaptively estimates from the test signal the clutter subspace, which is in general distinct for different transmit/receive pairs and, moreover, may spread over the entire Doppler bandwidth. The second is a fully adaptive parametric detector which employs a parametric autoregressive clutter model and offers joint model order selection, clutter estimation/mitigation, and target detection in an integrated and fully adaptive process. Both detectors are developed within the generalized likelihood ratio test (GLRT) framework, obviating the need for training signals that are indispensable for conventional detectors but are difficult to obtain in practice due to clutter non-homogeneity. Numerical results indicate that the proposed training-free detectors offer improved detection performance over covariance matrix based detectors when the latter have a moderate amount of training signals.**

***Index Terms*—Moving target detection, distributed multi-input multi-output (MIMO) radar, moving platforms, sparsity, parametric methods.**

I. Introduction

Radars on multiple airborne or ground based moving platforms are of increasing interest in recent years, since they can be deployed in close proximity to the event under investigation and thus offer remarkable sensing opportunities [1]. For example, unmanned aerial vehicles (UAVs) based radars are expected to play an important role in disaster relief efforts by quickly flying to the impacted area and providing the most accurate and updated information [2]. In urban sensing environments, potential targets may be obscured by buildings and other man-made structures; with sensors on moving platforms, the subject area can be probed from more favorable positions to yield enhanced detectability [3]. Other applications of radar on moving platforms for military and civilian sensing operations can be found in, e.g., [4]–[6].

With multiple sensors, the system can be implemented as a multi-input multi-output (MIMO) radar with multiple transmit/receive (TX/RX) antennas using multiple waveforms, which offers several advantages over traditional array radar systems (e.g., [7]–[10]). There are two general configurations, namely co-located MIMO radars [8], where antennas within the TX or RX array are closed to each other relative to the target, and distributed MMO radar [10], where the antennas are widely separated to allow statistically independent observations of the target from multiple aspects (geometric diversity).

Here, we consider the moving target detection (MTD) problem in distributed MIMO radar. The problem has been studied in a number of studies leading to a sample covariance matrix (SCM) based detector [10], [11], a robust extension of the SCM based detector [12], [13], a subspace based detector [14], a parametric MTD detector [15], among others. However, all these studies were restricted to the case when radar platforms are non-moving. One major challenge of the MTD problem in distributed MIMO radar is clutter non-homogeneity. The covariance matrix based detectors in [10], [11], [16] can provide good performance only when adequate homogeneous training data is available, a condition that is difficult to meet in practice. As shown in Section II, the clutter in distributed MIMO radar is strongly location dependent, viz., it depends on the location of the test cell relative to the geometry of the transmit/receive (TX/RX) platforms as well as platform motion. As a result, the clutter covariance matrix varies significantly across resolution cells and dynamically changes over time. This non-homogeneity becomes even more severe when the moving platforms operate in complex environments such as urban areas or mountainous terrains. Due to the location-dependent characteristics, the clutter observed by each TX/RX pair in the same resolution cell may also have very different non-homogeneous covariance structure than other pairs.

To handle such clutter non-homogeneity, a subspace MIMO detector is proposed in [14], which uses only the test signal for detection and does not require any range training data. However, the subspace clutter model is based on the assumption that the clutter Doppler frequencies are centered around zero. This assumption is valid only when the platforms are non-moving, in which case the clutter Doppler effect is caused by natural phenomena such as wind, rain, and current flow/wave in rivers/oceans, etc. With moving platforms, the clutter Doppler frequency may spread over the entire Doppler bandwidth, which disqualifies the subspace detector.

H. Li and Z. Wang are with the Department of Electrical and Computer Engineering, Stevens Institute of Technology, Hoboken, NJ 07030, USA (e-mails: Hongbin.Li@stevens.edu, zwang23@stevens.edu).

J. Liu was with the Department of Electrical and Computer Engineering, Stevens Institute of Technology. He is now with the National Laboratory of Radar Signal Processing, Xidian University, Xi'an, 710071, China (e-mail: jun_liu_math@hotmail.com).

B. Himed is with AFRL/RYMD, Dayton, OH 45433 USA (e-mail: braham.himed@us.af.mil).

This article has been accepted for publication in a future issue of this journal, but has not been fully edited. Content may change prior to final publication. Citation information: DOI 10.1109/JSTSP.2015.2467355, IEEE Journal of Selected Topics in Signal Processing

Meanwhile, a parametric MIMO detector is introduced in [15]. The detector circumvents the need for range training data by utilizing low-order autoregressive (AR) processes for clutter modeling and estimation. While this offers an effective approach to mitigate clutter non-homogeneity, the limitation of [15] is that the model orders of the AR processes are assumed to be available a priori. The assumption is justified only with non-moving radar platforms, in which case the clutter is stationary or slowly changing over time, and the clutter model order can be estimated in advance. In [12], [13], a compound Gaussian model is used to describe the non-homogeneity of clutter. This leads to a modified covariance matrix based detector with improved performance than those of [10], [11], [16] in non-homogenous clutter environments. Nevertheless, the detector still requires a substantial amount of training data for covariance matrix estimation.

In this paper, we address the MTD problem with explicit consideration of platform motion. We first analyze target and clutter responses in a multistatic setup and highlight the effects of platform motion, which exacerbate the non-homogeneous clutter problem. Based on the analysis, we develop new detection algorithms by integrating and extending recent developments in sparse signal recovery and previous MTD solutions [14], [15]. Specifically, two detectors are developed, namely a sparsity based detector and a fully adaptive parametric detector. The former exploits a sparse representation of the clutter. Unlike [14] where the clutter subspace is assumed known, identical for all TX/RX pairs, and covering only a small fractional of the Doppler bandwidth around zero frequency, the sparsity based detector is able to adaptively estimate the clutter subspace including its rank from a dictionary matrix that spans the Doppler bandwidth, and the clutter subspace is generally distinct for different TX/RX pairs and may spread over the entire frequency domain. Meanwhile, the fully adaptive parametric detector extends [15] by incorporating adaptive model order selection in the detection process to cope with platform motion. Both detectors are developed within the generalized likelihood ratio test (GLRT) framework, through which the clutter can be estimated from only the test signal under the null and alternative hypothesis, respectively, without using any range training signals. It should be noted that the range training-free feature stems from the sparsity/parametric based models employed by these detectors. The estimation results are then contrasted with each other and the one not matched to the real hypothesis is rejected through GLRT. Computer simulation show that these training-free detectors significantly outperform the covariance matrix based detectors when the latter are provided with a moderate amount of range training in the considered MTD environment with moving platforms.

The remainder is organized as follows. In Section II, we present the geometry of the distributed MIMO radar with moving platforms, examine the target/clutter responses, and formulate the MTD problem. In Section III, we briefly review several existing MTD detectors and discuss their related problems. The proposed detectors are developed in Section IV. Numerical results and comparisons are presented in Section V, followed by concluding remarks in Section VI.

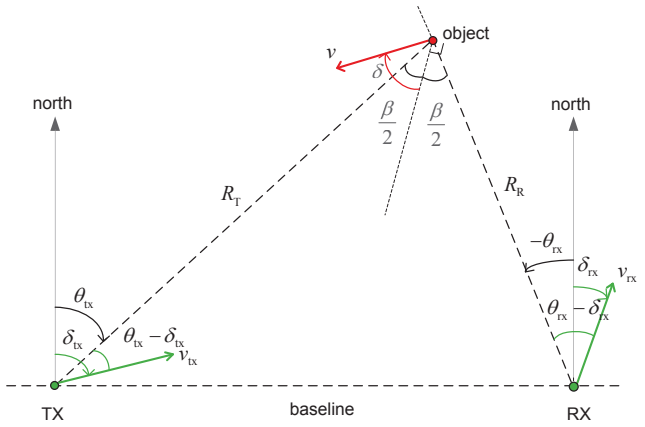

Fig. 1. Bistatic geometry involving one TX, one RX, and one object (target or clutter scatterer).

II. Data Model and Problem Formulation

A. Bistatic Geometry and Doppler Frequency

In this subsection, we examine the bistatic geometry of a single transmitter (TX) and receiver (RX) on moving platforms and the resulting Doppler frequency of a moving object observed by the TX-RX pair. The result is used to develop a data model for the MIMO case in Section II-B. Fig. 1 shows the bistatic geometry of an object that forms a bistatic angle β with the TX-RX pair. For simplicity, we assume the TX, RX and the object are located on a two-dimensional (2-D) plane. The object may refer to a moving target with speed v and moving direction δ with respect to (w.r.t.) the bisector of β; or it may refer to a clutter scatterer in which case $v = 0$. The moving angles of the TX and RX are denoted by δ_{tx} and δ_{rx}, while their look angles are θ_{tx} and θ_{rx}, respectively, all defined w.r.t. the North direction. The *transmit range* (TX-to-object) is denoted by R_{T}, while the *receive range* (object-to-RX) by R_{R}. Note that all angles in Fig. 1 have signs, with clockwise being positive and counter-clockwise being negative.

Based on the above bistatic radar geometry, the bistatic Doppler frequency of the moving object is the time rate of change of the total TX-RX path length [17]:

$$f = \frac{1}{\lambda}\left[\frac{dR_{\text{T}}}{dt} + \frac{dR_{\text{R}}}{dt}\right], \tag{1}$$

where λ denotes the wavelength, $\frac{dR_{\text{T}}}{dt}$ and $\frac{dR_{\text{R}}}{dt}$ are the *relative velocities* for the TX and RX, respectively. They can be treated as the projections of v_{tx} and v_{rx} onto R_{T} and R_{R}:

$$\frac{dR_{\text{T}}}{dt} = v_{\text{tx}}\cos(\delta_{\text{tx}} - \theta_{\text{tx}}) + v\cos(\delta - \frac{\beta}{2}), \tag{2}$$

$$\frac{dR_{\text{R}}}{dt} = v_{\text{rx}}\cos(\delta_{\text{rx}} - \theta_{\text{rx}}) + v\cos(\delta + \frac{\beta}{2}). \tag{3}$$

Taking (2) and (3) back into (1), we have

$$f = \frac{1}{\lambda}\left[2v\cos\delta\cos\frac{\beta}{2} + v_{\text{tx}}\cos(\delta_{\text{tx}} - \theta_{\text{tx}}) + v_{\text{rx}}\cos(\delta_{\text{rx}} - \theta_{\text{rx}})\right], \tag{4}$$

which reveals that f consists of three parts due to the motion of the object, and the motion of the TX/RX. Several cases of practical interest are worth discussing.

This article has been accepted for publication in a future issue of this journal, but has not been fully edited. Content may change prior to final publication. Citation information: DOI 10.1109/JSTSP.2015.2467355, IEEE Journal of Selected Topics in Signal Processing

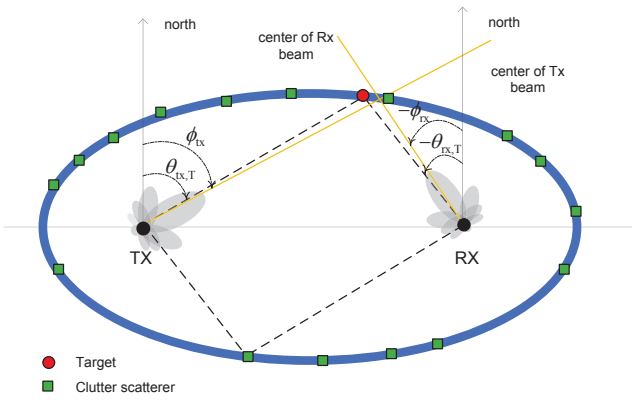

Fig. 2. Bistatic geometry and isorange.

1) Moving object and stationary platforms: With $v_{\text{tx}} = v_{\text{rx}} = 0$, (4) reduces to

$$f = \frac{1}{\lambda}\left(2v\cos\delta\cos\frac{\beta}{2}\right). \tag{5}$$

This is the case examined in [11], [14]. It can be seen from (5) that the Doppler frequency is only dependent on the object motion and the bistatic angle $\beta \in [0°, 180°]$. From fixed target motion, the Doppler frequency becomes larger as β decreases. Note that (5) also holds with moving platforms when their moving angles are perpendicular to their look angles, i.e., $\delta_{\text{tx}} - \theta_{\text{tx}} = \pm 90°$ and $\delta_{\text{rx}} - \theta_{\text{rx}} = \pm 90°$.

2) Stationary object and moving platforms: When the object is stationary ($v = 0$), for fixed target motion, the Doppler frequency is caused by the motion of the platforms:

$$f = \frac{1}{\lambda}\left[v_{\text{tx}}\cos(\delta_{\text{tx}} - \theta_{\text{tx}}) + v_{\text{rx}}\cos(\delta_{\text{rx}} - \theta_{\text{rx}})\right]. \tag{6}$$

The above equation is useful for determining the Doppler frequency of a clutter scatterer.

3) Moving object on the baseline: When the target is on the baseline ($\beta = 180°$), (4) reduces to (6) as well, and the Doppler frequency is contributed only by the platform motion. In such cases the target cannot be detected by the radar.

4) Monostatic Radar: For monostatic radar, we have $\beta = 0°$, $v_{\text{tx}} = v_{\text{rx}}$, $\delta_{\text{tx}} = \delta_{\text{rx}}$ and $\theta_{\text{tx}} = \theta_{\text{rx}}$. The Doppler frequency reduces to

$$f = \frac{2}{\lambda}\left[v\cos\delta + v_{\text{tx}}\cos(\delta_{\text{tx}} - \theta_{\text{tx}})\right], \tag{7}$$

which, in comparison with (4), shows that for the same target/platform motion, the Doppler frequency of a monostatic radar is always lager than that of a bistatic radar.

B. Target and Clutter Model

Consider a distributed MIMO radar system with M TXs and N RXs, possibly moving, which forms a total of MN bistatic pairs. As in standard radar operation, the radar scene is divided into multiple resolution cells, the cell size is determined by the bandwidth and beamwidth of the radar system, and detection is performed on each cell one by one to look for moving targets of interest [18], [19]. For a given resolution cell under investigation (called *test cell*), let R_{T} and R_{R} be the associated transmit and, respectively, receive range. The *range sum* $R_{\text{T}} + R_{\text{R}}$ defines an *isorange* of the bistatic triangle, which is an ellipse with foci at the TX and RX [17], as shown in Fig. 2.

Suppose each TX sends a succession of K periodic pulses, i.e., K repetitions of an orthogonal waveform over a coherent processing interval (CPI) [10], [11]. Each RX employs a bank of M matched filters corresponding to the M TX waveforms. The matched filter outputs are sampled at the pulse rate with suitable delays according to the range sum of the test cell. Let $\mathbf{x}_{mn}$ denote the vector formed by the $K \times 1$ samples of the matched filter output in one CPI at the n-th RX matched to the m-th TX waveform. $\mathbf{x}_{mn}$ is the test signal, which includes contributions from the target (if present) and clutter scatterers located on the isorange associated with the test cell, i.e., the ellipse shown in Fig. 2.

1) Target response: The target response in the test signal $\mathbf{x}_{mn}$ can be written as $\alpha_{mn}\mathbf{s}_{mn}$, where α_{mn} denotes the unknown complex-valued target amplitude and $\mathbf{s}_{mn}$ the target *steering vector* [11], [18]:

$$\mathbf{s}_{mn}(v,\delta) = \left[1 \quad e^{-\jmath 2\pi T_{\text{p}} f_{mn}} \quad \dots \quad e^{-\jmath 2\pi (K-1) T_{\text{p}} f_{mn}}\right]^{\text{T}}, \tag{8}$$

where T_{p} is the pulse repetition interval (PRI), and f_{mn} is the target Doppler frequency that is a function of the target speed v and the moving direction δ [cf. Fig. 1 and (4)], and is assumed to remain fixed within a CPI. The target amplitude is determined by a number of factors such as the transmit power, antenna gain pattern, and the radar cross section (RCS) of the target [17], [19]. Specifically, consider Fig. 2 which depicts a target being illuminated by a transmit beam with look angle ϕ_{tx} and observed by a receive beam with look angle ϕ_{rx}. The target amplitude can be expressed as[1]

$$\alpha_{mn} \propto \frac{\rho}{R_{\text{T}} R_{\text{R}}}\sqrt{P G_{\text{tx}}(\theta_{\text{tx,T}} - \phi_{\text{tx}}) G_{\text{rx}}(\theta_{\text{rx,T}} - \phi_{\text{rx}})}, \tag{9}$$

where ρ is a complex-valued parameter determined by the radar RCS and channel-induced phase shift, P denotes the radar transmit power, $G_{\text{tx}}(\theta_{\text{tx,T}} - \phi_{\text{tx}})$ and $G_{\text{rx}}(\theta_{\text{rx,T}} - \phi_{\text{rx}})$ are the TX and RX gain patterns which depend on the target locations angles $\theta_{\text{tx,T}}$ and $\theta_{\text{rx,T}}$, relative to TX/RX look angles ϕ_{tx} and ϕ_{rx}, as shown in Fig. 2.

2) Clutter response: The clutter response in the test signal $\mathbf{x}_{mn}$ is the sum of reflections from all clutter scatterers on the bistatic isorange as shown in Fig. 2. Assuming there are L_{mn} dominant clutter scattering points on the isorange, the clutter response can be approximated as [18, Section 2.6]:

$$\mathbf{c}_{mn} = \sum_{i=1}^{L_{mn}} \gamma_{mn,i}\mathbf{h}(f_{mn,i}), \tag{10}$$

[1]It should be noted that many quantities involved here depend on m, n, or both. For example, the transmission power P may be expressed as P_m as it relates to the m-th TX, the receive beam pattern $G_{\text{rx}}(\cdot,\cdot)$ may be written as $G_{\text{rx},n}(\cdot,\cdot)$ as it is associated with the n-th RX, and the target RCS ρ also depends on the (m,n)-th pair, etc. Since it is clear from the context, the dependence is suppressed for notational brevity. Meanwhile, we keep the subscript mn for α_{mn} and other similar quantities since they are used in later sections.

This article has been accepted for publication in a future issue of this journal, but has not been fully edited. Content may change prior to final publication. Citation information: DOI 10.1109/JSTSP.2015.2467355, IEEE Journal of Selected Topics in Signal Processing

where $\gamma_{mn,i}$ denotes the clutter amplitude associated with the i-th scatterer, and $\mathbf{h}(f_{mn,i})$ is the corresponding clutter Doppler steering vector given by

$$\mathbf{h}(f_{mn,i}) = [1 \quad e^{-\jmath 2\pi T_{\mathrm{p}} f_{mn,i}} \quad ... \quad e^{-\jmath 2\pi (K-1) T_{\mathrm{p}} f_{mn,i}}]^{\mathrm{T}}, \tag{11}$$

where $f_{mn,i}$ denotes the Doppler frequency associated with the i-th clutter scatterer, which is assumed to be fixed during a CPI. From (6), the Doppler frequency is determined by the platform motion as well as the location of the clutter scatterer relative to the platforms. Similar to the target amplitude (9), the clutter amplitude $\gamma_{mn,i}$ has a dependence on the transmit power, antenna gain, and transmit/receive range associated with the clutter scatterer (cf. Fig. 2):

$$\gamma_{mn,i} \propto \frac{\rho}{R_{\mathrm{T}} R_{\mathrm{R}}} \sqrt{P G_{\mathrm{tx}}(\theta_{\mathrm{tx,c},i} - \phi_{\mathrm{tx}}) G_{\mathrm{rx}}(\theta_{\mathrm{rx,c},i} - \phi_{\mathrm{rx}})}, \tag{12}$$

where $\theta_{\mathrm{tx,c},i}$ and $\theta_{\mathrm{rx,c},i}$ denote the location angles of the i-th clutter scatterer.

C. Detection Problem

Given the discussions in previous sub-sections, the moving target detection problem using M TXs and N RXs can be formulated as the following composite hypothesis test:

$$\begin{aligned} H_0: \quad & \mathbf{x}_{mn} = \mathbf{c}_{mn} + \mathbf{n}_{mn}, \\ H_1: \quad & \mathbf{x}_{mn} = \alpha_{mn} \mathbf{s}_{mn}(v,\delta) + \mathbf{c}_{mn} + \mathbf{n}_{mn}, \\ & m = 1, 2, \cdots, M; \ n = 1, 2, \cdots, N, \end{aligned} \tag{13}$$

where $\mathbf{x}_{mn}$ denotes the test signal observed from the (m,n)-th TX-RX pair; $\mathbf{s}_{mn}(v,\delta)$ is the target steering vector which depends on the unknown target speed v and direction δ as in (8), α_{mn} is the unknown target amplitude, $\mathbf{c}_{mn}$ is the clutter given by (10) which involves unknown parameters including the number of clutter points $\{L_{mn}\}$, clutter amplitudes $\{\gamma_{mn,i}\}$ and Doppler frequencies $\{f_{mn,i}\}$; finally, $\mathbf{n}_{mn}$ is the noise, which is modeled as uncorrelated Gaussian with zero mean and variance σ_{mn}^2. The problem of interest is to detect the presence/absence of the moving target using the observed signals $\{\mathbf{x}_{mn}\}$.

III. Covariance Matrix Based Detectors

Let

$$\mathbf{d}_{mn} = \mathbf{c}_{mn} + \mathbf{n}_{mn}, \tag{14}$$

which is often referred to as the *disturbance* signal. A standard approach is to model the disturbance as Gaussian with zero mean and covariance matrix $\mathbf{R}_{mn} = \mathbf{R}_{\mathrm{c},mn} + \sigma_{mn}^2 \mathbf{I}$, where $\mathbf{R}_{\mathrm{c},mn}$ denotes the clutter covariance matrix. If $\mathbf{R}_{mn}$ is known, then from the perspective of maximizing the output signal-to-clutter-plus-noise ratio (SCNR), the optimum detector is the matched filter (MF) [18]:

$$T_{\mathrm{MF}} = \sum_{m=1}^{M} \sum_{n=1}^{N} \frac{|\mathbf{s}_{mn}^{\mathrm{H}} \mathbf{R}_{mn}^{-1} \mathbf{x}_{0,mn}|^2}{\mathbf{s}_{mn}^{\mathrm{H}} \mathbf{R}_{mn}^{-1} \mathbf{s}_{mn}}. \tag{15}$$

In practice, the covariance matrix $\mathbf{R}_{mn}$ is unknown and needs to be estimated. A popular choice is the *sample covariance matrix*:

$$\hat{\mathbf{R}}_{mn} = \frac{1}{T} \sum_{t=1}^{T} \mathbf{x}_{mn,t} \mathbf{x}_{mn,t}^{\mathrm{H}}, \tag{16}$$

where $\mathbf{x}_{mn,t}$ denotes the training signals associated with the test signal $\mathbf{x}_{mn}$. Replacing $\mathbf{R}_{mn}$ by the $\hat{\mathbf{R}}_{mn}$ leads to the the SCM based detector [10], [11]:

$$T_{\mathrm{SCM}} = \max_{v,\delta} \sum_{m=1}^{M} \sum_{n=1}^{N} \frac{|\mathbf{s}_{mn}^{\mathrm{H}}(v,\delta) \hat{\mathbf{R}}_{mn}^{-1} \mathbf{x}_{0,mn}|^2}{\mathbf{s}_{mn}^{\mathrm{H}}(v,\delta) \hat{\mathbf{R}}_{mn}^{-1} \mathbf{s}_{mn}(v,\delta)}. \tag{17}$$

To ensure that $\hat{\mathbf{R}}_{mn}$ has full rank, $T > K$ training data are required for each TX-RX pair. In general, $T \geq 2K$ training data are needed for an acceptable performance [18]. Therefore, the SCM detector in (17) requires roughly $2KMN$ training data in total.

Another detector for MTD with distributed MIMO radar is the robust SCM detector [12], [13]

$$T_{\text{robust-SCM}} = \max_{v,\delta} \prod_{mn} \left[1 - \frac{|\mathbf{s}_{mn}^{\mathrm{H}}(v,\delta) \hat{\mathbf{M}}_{mn}^{-1} \mathbf{x}_{mn}|^2}{\left(\mathbf{s}_{mn}^{\mathrm{H}}(v,\delta) \hat{\mathbf{M}}_{mn}^{-1} \mathbf{s}_{mn}(v,\delta)\right) \left(\mathbf{x}_{mn}^{\mathrm{H}} \hat{\mathbf{M}}_{mn}^{-1} \mathbf{x}_{mn}\right)} \right]^{-K}, \tag{18}$$

where $\hat{\mathbf{M}}_{mn}$ is a fixed point estimate (FPE) of the covariance matrix by solving [20]–[22]

$$\hat{\mathbf{M}}_{mn} = \frac{K}{T} \sum_{t=1}^{T} \frac{\mathbf{x}_{mn,t} \mathbf{x}_{mn,t}^{\mathrm{H}}}{\mathbf{x}_{mn,t}^{\mathrm{H}} \hat{\mathbf{M}}_{mn}^{-1} \mathbf{x}_{mn,t}}. \tag{19}$$

The above robust SCM detector is based on a compound-Gaussian model for the test signals across TX-RX pairs. It requires training signals which follow the same compound-Gaussian model. The FPE (19) can be obtained using an iterative approach [20]–[22].

The above solutions assume the availability of some training signals, which are often collected in the neighboring resolution cells close to the test cell [18], [19]. This causes some problems. In particular, from Section II-B it is clear that the clutter response vector (both the amplitude and Doppler frequency) is location dependent, i.e., the clutter at different resolution cells or TX-RX pairs exhibits different clutter characteristics. The location-dependent clutter characteristics lead to two types of non-homogeneities. First, for the same resolution cell, the clutter observed by different TX-RX pair is non-homogeneous, i.e., $\mathbf{R}_{mn} \neq \mathbf{R}_{m'n'}$, if $m \neq m'$ and/or $n \neq n'$. Second, for different resolution cells, the covariance matrix is also different. Hence, drawing training data from the neighboring range cells for covariance matrix estimation, as done by the conventional detectors, may suffer significant performance degradation due to the non-homogeneous nature of the clutter in distributed MIMO radar. It is therefore imperative to seek alternative detectors with reduced training signals.

This article has been accepted for publication in a future issue of this journal, but has not been fully edited. Content may change prior to final publication. Citation information: DOI 10.1109/JSTSP.2015.2467355, IEEE Journal of Selected Topics in Signal Processing

IV. Proposed Approaches

In this section, we propose two detectors which do not require range training data. The first detector as introduced in Section IV-A exploits a sparsity based model to mitigate the principal clutter responses, while the second one in Section IV-B is based on a parametric clutter modeling approach. In the development of these detectors, we assume the target velocity is known for simplicity and drop the dependence of the target steering vectors $\{\mathbf{s}_{mn}\}$ on $\{v, \delta\}$. It is standard in radar detection to divide the uncertainty region of the target velocity into small cells and each is tested for the presence of the target [18]. The problem of estimating the target velocity parameters $\{v, \delta\}$ is addressed in Section IV-C.

A. Sparsity Based Detector

Herein, we present a detector which aims to reject the clutter response from the dominant clutter scatterers in the test cell. In practice, the dominant clutter scatterers which have the most impact must be effectively rejected to expose the target for detection. The clutter from the dominant scatterers in the test cell can be considered as residing in a subspace which can be expanded by the columns of a matrix $\mathbf{H}_{mn} \in C^{K \times L_{mn}}$ [18]

$$\mathbf{H}_{mn} = \left[\mathbf{h}(f_1), \mathbf{h}(f_2), \cdots, \mathbf{h}(f_{L_{mn}})\right], \tag{20}$$

where

$$\mathbf{h}(f_i) = \left[1, e^{-\jmath 2\pi T_{\mathrm{p}} f_i}, \cdots, e^{-\jmath 2\pi (K-1) T_{\mathrm{p}} f_i}\right]^{\mathrm{T}}, \tag{21}$$

with f_i representing the Doppler frequency of the i-th clutter scattering point. Then, the clutter response vector for the (m,n)-th TX-RX pair in (10) can be rewritten in matrix form

$$\mathbf{c}_{mn} = \sum_{i=1}^{L_{mn}} \gamma_{mn,i} \mathbf{h}(f_i) = \mathbf{H}_{mn} \boldsymbol{\gamma}_{mn}, \tag{22}$$

where $\mathbf{H}_{mn}$ represents the subspace of the clutter observed at the (m,n)-th TX-RX pair and $\boldsymbol{\gamma}_{mn}$ is an $L_{mn} \times 1$ vector containing the *unknown* complex clutter coefficients.

Substituting (22) into (13), the hypothesis testing problem is rewritten as follows

$$\begin{aligned} H_0: &\quad \mathbf{x}_{mn} = \mathbf{H}_{mn}\boldsymbol{\gamma}_{mn} + \mathbf{n}_{mn}, \\ H_1: &\quad \mathbf{x}_{mn} = \alpha_{mn}\mathbf{s}_{mn} + \mathbf{H}_{mn}\boldsymbol{\gamma}_{mn} + \mathbf{n}_{mn}, \end{aligned} \tag{23}$$

where $\mathbf{n}_{mn}$ is additive white Gaussian noise with zero mean and variance σ_{mn}^2. The likelihood functions p_i ($i = 1$ for H_1 and $i = 0$ for H_0) are given by

$$\begin{aligned} H_0: &\quad p_0\left(\mathbf{x}_{mn}; \mathbf{H}_{mn}, \boldsymbol{\gamma}_{mn}, \sigma_{mn}^2\right) \\ &= \frac{\exp\left(-\frac{1}{\sigma_{mn}^2}\|\mathbf{x}_{mn} - \mathbf{H}_{mn}\boldsymbol{\gamma}_{mn}\|^2\right)}{\left(\pi\sigma_{mn}^2\right)^K}, \\ H_1: &\quad p_1\left(\mathbf{x}_{mn}; \alpha_{mn}, \mathbf{H}_{mn}, \boldsymbol{\gamma}_{mn}, \sigma_{mn}^2\right) \\ &= \frac{\exp\left(-\frac{1}{\sigma_{mn}^2}\|\mathbf{x}_{mn} - \alpha_{mn}\mathbf{s}_{mn} - \mathbf{H}_{mn}\boldsymbol{\gamma}_{mn}\|^2\right)}{\left(\pi\sigma_{mn}^2\right)^K}. \end{aligned} \tag{24, 25}$$

We consider a generalized likelihood ratio test (GLRT) approach for target detection. The test variable of the GLRT is given by the ratio of the likelihood function with unknowns replaced by their maximum likelihood estimates (MLEs) [23]

$$T'_{\text{S-GLRT}} = \frac{\prod_{mn} \max_{\alpha_{mn}, \mathbf{H}_{mn}, \boldsymbol{\gamma}_{mn}, \sigma_{mn}^2} p_1\left(\alpha_{mn}, \mathbf{H}_{mn}, \boldsymbol{\gamma}_{mn}, \sigma_{mn}^2\right)}{\prod_{mn} \max_{\mathbf{H}_{mn}, \boldsymbol{\gamma}_{mn}, \sigma_{mn}^2} p_0\left(\mathbf{H}_{mn}, \boldsymbol{\gamma}_{mn}, \sigma_{mn}^2\right)}. \tag{26}$$

Next, we discuss how to obtain the parameter estimates under both the H_1 and H_0 hypotheses, respectively.

1) Parameter Estimation under H_1: From (25), the MLE of the target amplitude α_{mn} conditioned on $\mathbf{H}_{mn}$ and $\boldsymbol{\gamma}_{mn}$ is

$$\hat{\alpha}_{mn} = \frac{\mathbf{s}_{mn}^{\mathrm{H}}\left(\mathbf{x}_{mn} - \mathbf{H}_{mn}\boldsymbol{\gamma}_{mn}\right)}{\mathbf{s}_{mn}^{\mathrm{H}}\mathbf{s}_{mn}}. \tag{27}$$

Substituting (27) into (25) and maximizing the resulting likelihood function w.r.t. σ_{mn}^2, we obtain the MLE for the noise variance σ_{mn}^2 conditioned on $\mathbf{H}_{mn}$, $\boldsymbol{\gamma}_{mn}$ and $\hat{\alpha}_{mn}$, which is

$$\hat{\sigma}_{mn:1}^2 = \frac{\|\mathbf{y}_{mn} - \mathbf{P}_{mn}^{\perp}\mathbf{H}_{mn}\boldsymbol{\gamma}_{mn}\|^2}{K}, \tag{28}$$

where

$$\mathbf{P}_{mn}^{\perp} = \mathbf{I} - \frac{\mathbf{s}_{mn}\mathbf{s}_{mn}^{\mathrm{H}}}{\mathbf{s}_{mn}^{\mathrm{H}}\mathbf{s}_{mn}}, \tag{29}$$

$$\mathbf{y}_{mn} = \mathbf{P}_{mn}^{\perp}\mathbf{x}_{mn}. \tag{30}$$

By substituting (27) and (28) into (25), the maximization of the likelihood function w.r.t. the clutter parameters reduces to

$$\{\hat{\mathbf{H}}_{mn}, \hat{\boldsymbol{\gamma}}_{mn}\} = \arg \min_{\mathbf{H}_{mn}, \boldsymbol{\gamma}_{mn}} \|\mathbf{y}_{mn} - \mathbf{P}_{mn}^{\perp}\mathbf{H}_{mn}\boldsymbol{\gamma}_{mn}\|^2. \tag{31}$$

Note that (31) is a non-linear estimation problem, which jointly estimates the clutter subspace $\mathbf{H}_{mn}$ parameterized by the Doppler frequencies $\{f_i\}_{i=1}^{L_{mn}}$ and amplitudes $\boldsymbol{\gamma}_{mn}$. This non-linear estimation problem can be linearized using an *overcomplete* dictionary matrix

$$\bar{\mathbf{H}} = \left[\mathbf{h}(\bar{f}_1), \mathbf{h}(\bar{f}_2), \cdots, \mathbf{h}(\bar{f}_D)\right], \tag{32}$$

with the dimension $D \gg K$, where $\{\bar{f}_i\}$ are a set of uniformly spaced frequency points covering the entire Doppler spectrum. For sufficiently large D, i.e., the Doppler spectrum is densely sampled, the clutter response can be written as

$$\mathbf{H}_{mn}\boldsymbol{\gamma}_{mn} = \bar{\mathbf{H}}\bar{\boldsymbol{\gamma}}_{mn}, \tag{33}$$

where $\bar{\boldsymbol{\gamma}}_{mn}$ is a $D \times 1$ sparse vector with only L_{mn} non-zero elements (the locations of the non-zero elements are however unknown). The non-linear joint estimation problem (31) now reduces to a sparse linear parameter estimation problem, i.e., to estimate the linear amplitude vector $\bar{\boldsymbol{\gamma}}_{mn}$, under a sparsity constraint. Therefore (31) is equivalent to

$$\begin{aligned} \hat{\bar{\boldsymbol{\gamma}}}_{mn} &= \arg \min_{\bar{\boldsymbol{\gamma}}_{mn}} \|\mathbf{y}_{mn} - \mathbf{P}_{mn}^{\perp}\bar{\mathbf{H}}\bar{\boldsymbol{\gamma}}_{mn}\|^2, \\ &\text{s.t.} \quad \|\bar{\boldsymbol{\gamma}}_{mn}\|_0 = L_{mn}, \end{aligned} \tag{34}$$

where $\|\cdot\|_0$ denotes the L_0-norm of a vector argument which gives the total number of non-zero elements in the vector.

Finding the exact MLE of $\bar{\boldsymbol{\gamma}}_{mn}$ is combinatorial. Specifically, we need to minimize the cost function of (34) for every combination of L_{mn} columns of $\bar{\mathbf{H}}$ that have non-zero coefficients, i.e., we have to solve $\binom{D}{L_{mn}}$ least-squares (LS)

This article has been accepted for publication in a future issue of this journal, but has not been fully edited. Content may change prior to final publication. Citation information: DOI 10.1109/JSTSP.2015.2467355, IEEE Journal of Selected Topics in Signal Processing

problems, which is highly complex for large D. Instead of the exact MLE, we can obtain an approximate estimate of $\bar{\boldsymbol{\gamma}}_{mn}$ by resorting to standard sparse signal recovery methods with small-to-moderate complexities, such as the greedy methods [24] or convex relaxation based methods [25]. Next, we discuss how to employ the orthogonal matching pursuit (OMP) [24] to estimate $\bar{\boldsymbol{\gamma}}_{mn}$ due to its computational efficiency, and we also discuss how to address the issue when the sparsity L_{mn}, i.e., the dimension of the clutter subspace, is unknown.

To facilitate discussion, let $\mathbf{b} = \mathbf{y}_{mn}$, $\mathbf{A} = \mathbf{P}_{mn}^{\perp}\bar{\mathbf{H}}$, $\bar{\boldsymbol{\gamma}}_{mn} = \mathbf{z}$, and $L_{mn} = L$. Then (34) can be rewritten as

$$\begin{aligned} \hat{\mathbf{z}} &= \arg\min_{\mathbf{z}} \|\mathbf{b} - \mathbf{A}\mathbf{z}\|^2, \\ &\text{s.t.} \quad \|\mathbf{z}\|_0 = L. \end{aligned} \tag{35}$$

The idea is to iteratively identify an atom (i.e., a column) of $\mathbf{A}$ at a time that has the largest correlation with the residual vector until convergence. Specifically, denote by $\Gamma = \{1, 2, \cdots, D\}$ the index set of all atoms of $\mathbf{A}$, Λ_t the correlation index set containing the indices of the identified atoms of $\mathbf{A}$ at the t-th iteration, and $\mathbf{r}_t$ the $K \times 1$ residual vector obtained after subtracting the contribution from the identified atoms at the t-th iteration. To initialize the iterative process, we set $\Lambda_0 = \emptyset$ and $\mathbf{r}_0 = \mathbf{b}$. At the t-th iteration, a new atom is identified from the remaining atoms of $\mathbf{A}$ that has the largest correlation with the residual $\mathbf{r}_{t-1}$:

$$\lambda_t = \arg\max_{j \in \Gamma \setminus \Lambda_{t-1}} |\mathbf{r}_{t-1}^{\mathrm{H}} \mathbf{A}(:, j)|, \tag{36}$$

where $\mathbf{A}(:, j)$ denotes the j-th column of $\mathbf{A}$. Then, the correlation index set and residual are updated as follows:

$$\Lambda_t = \Lambda_{t-1} \cup \{\lambda_t\}, \tag{37}$$

$$\mathbf{r}_t = \mathbf{b} - \mathbf{A}(:, \Lambda_t)\hat{\mathbf{z}}_t, \tag{38}$$

where $\mathbf{A}(:, \Lambda_t)$ denotes the $K \times t$ sub-matrix formed by the columns of $\mathbf{A}$ as indexed by the correlation index set Λ_t and

$$\hat{\mathbf{z}}_t = \mathbf{A}(:, \Lambda_t)^{\dagger}\mathbf{b}, \tag{39}$$

where $(\cdot)^{\dagger}$ denotes the matrix pseudo-inverse. The iterative process stops when the following criterion is met:

$$\max_{j \in \Gamma \setminus \Lambda_{t-1}} \frac{|\mathbf{r}_t^{\mathrm{H}} \mathbf{A}(:, j)|}{\|\mathbf{A}^{\mathrm{H}}\mathbf{b}\|_1} < \epsilon, \tag{40}$$

where ϵ is a small positive number which controls the dimension of the clutter subspace. Note that the left side of (40) measures the relative correlation between the residual and the remaining atoms at t-th iteration, and we have found a choice of $\epsilon = 10^{-3}$ is effective in suppressing the dominant clutter.

Suppose the iterative process stops at the t-th iteration. We have estimates of the clutter subspace and coefficients, $\hat{\mathbf{H}}_{mn} = \bar{\mathbf{H}}(:, \Lambda_t)$ and $\hat{\bar{\boldsymbol{\gamma}}}_{mn}(\Lambda_t) = \hat{\mathbf{z}}_t$, respectively, which are specified over the non-zero support Λ_t, and an estimate of the clutter rank is $\hat{L}_{mn} = t$. Substituting these estimates into (27) and (28), we can obtain estimates for the target amplitude and noise variance.

2) Parameter Estimation under H_0: Using a similar process, the MLE of noise variance conditioned on $\mathbf{H}_{mn}$ and $\boldsymbol{\gamma}_{mn}$ can be obtained from (24) as

$$\hat{\sigma}_{mn:0}^2 = \frac{\|\mathbf{x}_{mn} - \mathbf{H}_{mn}\boldsymbol{\gamma}_{mn}\|^2}{K}. \tag{41}$$

By taking (41) back into (24), the MLE of the clutter subspace matrix $\mathbf{H}_{mn}$ and amplitudes $\boldsymbol{\gamma}_{mn}$ are given by

$$\{\hat{\mathbf{H}}_{mn}, \hat{\boldsymbol{\gamma}}_{mn}\} = \arg\min_{\mathbf{H}_{mn}, \boldsymbol{\gamma}_{mn}} \|\mathbf{y}_{mn} - \mathbf{H}_{mn}\boldsymbol{\gamma}_{mn}\|^2, \tag{42}$$

which can be solved using the similar steps as shown in (35)-(40).

3) Test Statistic: Using the MLEs obtained above, it is straightforward to show that the GLRT test statistic reduces to

$$T_{\text{S-GLRT}} = \prod_{mn} \left(\frac{\hat{\sigma}_{mn:0}^2}{\hat{\sigma}_{mn:1}^2} \right)^K. \tag{43}$$

where $\hat{\sigma}_{mn:0}^2$ and $\hat{\sigma}_{mn:1}^2$ are the estimates of noise variance under H_0 and H_1, respectively.

- **Step A:** H_1 estimation
  1) Compute the projected signal $\mathbf{y}_{mn}$ from observations $\mathbf{x}_{mn}$, $m = 1, \ldots, M$, $n = 1, \ldots, N$, by (30).
  2) For each $\mathbf{y}_{mn}$, let $\mathbf{b} = \mathbf{y}_{mn}$ and $\mathbf{A} = \mathbf{P}_{mn}^{\perp}\bar{\mathbf{H}}$. Do the following iterations along with initializations: $\mathbf{r}_0 = \mathbf{y}_{mn}$, $\Lambda_0 = \emptyset$ and $t = 1$.
     a) Find the correlation index λ_t using (36), and update the correlation index set Λ_t using (37);
     b) Compute $\hat{\mathbf{z}}_t$ from (39), and update the residual vector $\mathbf{r}_t$ using (38);
     c) Check if the stop criterion (40) is met. If yes, move to Step A-3; otherwise, let $t = t + 1$, and go back to Step A-2a.
  3) Set the sparse clutter coefficient vector $\bar{\boldsymbol{\gamma}}_{mn}$ as $\hat{\bar{\boldsymbol{\gamma}}}(\Lambda_t) = \hat{\mathbf{z}}_t$ (over its non-zero support set Λ_t). Use it to compute an estimate of the clutter $\mathbf{H}_{mn}\boldsymbol{\gamma}_{mn}$ as $\bar{\mathbf{H}}\hat{\bar{\boldsymbol{\gamma}}}$ and, finally, an estimate of the noise variance $\hat{\sigma}_{mn:1}^2$ from (28).
- **Step B:** H_0 estimation
  1) For each $\mathbf{x}_{mn}$, let $\mathbf{b} = \mathbf{x}_{mn}$ and $\mathbf{A} = \bar{\mathbf{H}}$. Do the following iterations along with initializations: $\mathbf{r}_0 = \mathbf{x}_{mn}$, $\Lambda_0 = \emptyset$ and $t = 1$.
  2) Follow the same iterations from Step A-2a to Step A-2c.
  3) Calculate the estimates of clutter $\mathbf{H}_{mn}\boldsymbol{\gamma}_{mn}$ as in Step A-3 and the noise variance $\hat{\sigma}_{mn:0}^2$ from (41).
- **Step C:** Compute the test statistic from (43).

Algorithm 1: The proposed sparsity based detector.

A summary of the proposed sparsity based detector is included in Algorithm 1.

This article has been accepted for publication in a future issue of this journal, but has not been fully edited. Content may change prior to final publication. Citation information: DOI 10.1109/JSTSP.2015.2467355, IEEE Journal of Selected Topics in Signal Processing

B. Fully Adaptive Parametric Detector

In addition to the sparsity based model discussed in Section IV-A, parametric auto-regressive (AR) processes have proven useful to model radar clutter in various scenarios [26]–[37]. Examinations of numerous experimentally measured data have shown that AR processes can be used to accurately and efficiently approximate radar clutter using a few coefficients [28], [29], thus significantly reducing the amount of data that is needed for clutter estimation. For the detection problem at hand, consider the following P_{mn}-order AR process

$$d_{mn}(k) = -\sum_{p=1}^{P_{mn}} a_{mn}(p) d_{mn}(k-p) + \epsilon_{mn}(k), k = 1, 2, \cdots, K, \tag{44}$$

where $d_{mn}(k)$ denotes the k-th slow-time sample of the disturbance (clutter and noise) observed at the (m,n)-th TX-RX pair [cf. (14)], $a_{mn}(p)$ denotes the p-th AR coefficient of the AR process used to model $d_{mn}(k)$, and $\epsilon_{mn}(k) \sim \mathcal{CN}(0, \sigma_{mn}^2)$ is the driving noise of the AR process with zero-mean and variance σ_{mn}^2. The above AR model was employed in [15] for moving target detection when the radar platforms are stationary. A parametric detector was developed there under the assumption that the AR model orders $\{P_{mn}\}$ are given a priori. The assumption is justified since with fixed platforms, the environment is relatively stationary and the AR model orders $\{P_{mn}\}$ can be estimated a priori from previously collected data. As shown in Section II-B, the clutter response is location dependent. With moving platforms, the clutter is highly dynamic and changes rapidly over time, making it impossible to estimate $\{P_{mn}\}$ a priori. As such, for distributed MIMO radar on moving platforms, it is imperative to extend the parametric detector to provide joint adaptive model order estimation on the fly and moving target detection.

Using AR model (44), the likelihood function of the observed signal $\mathbf{x}_{mn}$ [see (13)] under hypothesis H_i, $i = 0$ or 1, is given by [15]

$$\begin{aligned} &p_i\left(a_{mn}(1), \cdots, a_{mn}(P_{mn}), \sigma_{mn}^2, \alpha_{mn}\right) \\ &= \frac{1}{\left(\pi\sigma_{mn}^2\right)^{K-P_{mn}}} \exp\left(-\frac{\sum_{k=P_{mn}+1}^{K} |\epsilon_{mn}(k)|^2}{\sigma_{mn}^2}\right) \end{aligned} \tag{45}$$

where $\alpha_{mn} = 0$ when $i = 0$, while $\epsilon_{mn}(k)$ are white Gaussian random variables which are related to the observed signal through the AR model:

$$H_0: \quad \epsilon_{mn}(k) = x_{mn}(k) + \sum_{p=1}^{P_{mn}} a_{mn}(p) x_{mn}(k-p), \tag{46}$$

$$\begin{aligned} H_1: \quad &\epsilon_{mn}(k) = x_{mn}(k) - \alpha_{mn} s_{mn}(k) \\ &+ \sum_{p=1}^{P_{mn}} a_{mn}(p) \left[x_{mn}(k-p) - \alpha_{mn} s_{mn}(k-p)\right], \\ &k = P_{mn}+1, P_{mn}+2, \cdots, K. \end{aligned} \tag{47}$$

Conditioned on known AR model orders $\{P_{mn}\}$, the MLEs of the target and disturbance parameters have been derived in [15]. The maximum logarithmic likelihood functions obtained by using these MLEs in (45) are [15, Eqs. (18) and (22)]:

$$H_0: \quad \ln p_0 \propto -(K - P_{mn}) \ln\left(\tilde{\mathbf{x}}_{mn}^{\mathrm{H}} \mathbf{P}_{\mathbf{Y}_{mn}}^{\perp} \tilde{\mathbf{x}}_{mn}\right), \tag{48}$$

$$H_1: \quad \ln p_1 \propto -(K - P_{mn}) \ln\left(\tilde{\mathbf{x}}_{mn}^{\mathrm{H}} \mathbf{P}_{\left[\mathbf{P}_{\psi_{mn}}^{\perp} \mathbf{Y}_{mn}\right]}^{\perp} \tilde{\mathbf{x}}_{mn}\right), \tag{49}$$

where $\tilde{\mathbf{x}}_{mn}$ is a vector formed from the observations $x_{mn}(k)$:

$$\tilde{\mathbf{x}}_{mn} = [x_{mn}(P_{mn}+1), x_{mn}(P_{mn}+2), \ldots, x_{mn}(K)]^{\mathrm{T}}, \tag{50}$$

$\mathbf{P}_{\mathbf{Y}_{mn}}^{\perp}$ and $\mathbf{P}_{\left[\mathbf{P}_{\psi_{mn}}^{\perp} \mathbf{Y}_{mn}\right]}^{\perp}$ are projection matrices given by

$$\mathbf{P}_{\mathbf{Y}_{mn}}^{\perp} = \mathbf{I} - \mathbf{Y}_{mn} \left(\mathbf{Y}_{mn}^{\mathrm{H}} \mathbf{Y}_{mn}\right)^{-1} \mathbf{Y}_{mn}^{\mathrm{H}}, \tag{51}$$

$$\begin{aligned} \mathbf{P}_{\left[\mathbf{P}_{\psi_{mn}}^{\perp} \mathbf{Y}_{mn}\right]}^{\perp} &= \mathbf{I} - \mathbf{P}_{\psi_{mn}}^{\perp} \mathbf{Y}_{mn} \\ &\times \left(\mathbf{Y}_{mn}^{\mathrm{H}} \mathbf{P}_{\psi_{mn}}^{\perp} \mathbf{Y}_{mn}\right)^{-1} \mathbf{Y}_{mn}^{\mathrm{H}} \mathbf{P}_{\psi_{mn}}^{\perp}, \end{aligned} \tag{52}$$

in which

$$\mathbf{Y}_{mn} = \begin{bmatrix} x_{mn}(P_{mn}) & \cdots & x_{mn}(1) \\ x_{mn}(P_{mn}+1) & \cdots & x_{mn}(2) \\ \vdots & \cdots & \vdots \\ x_{mn}(K-1) & \cdots & x_{mn}(K-P_{mn}) \end{bmatrix}, \tag{53}$$

$$\mathbf{P}_{\psi_{mn}}^{\perp} = \mathbf{I} - \frac{\boldsymbol{\psi}_{mn} \boldsymbol{\psi}_{mn}^{\mathrm{H}}}{\boldsymbol{\psi}_{mn}^{\mathrm{H}} \boldsymbol{\psi}_{mn}}, \tag{54}$$

where $\boldsymbol{\psi}_{mn} = \left[1, e^{\jmath 2\pi f_{mn}}, \cdots, e^{\jmath 2\pi (K-P_{mn}-1) f_{mn}}\right]^{\mathrm{T}}$ is a $(K - P_{mn}) \times 1$ Fourier vector.

We reiterate the above estimation results are based on known AR model orders $\{P_{mn}\}$, which need to be adaptively estimated from the observations. One naive way is to treat $\{P_{mn}\}$ are unknowns and directly maximize (48) and (49) w.r.t these parameters. This will inevitably lead to model over fitting, i.e., the resulting P_{mn} will always reach the maximum tested value [38]. There are a multitude of techniques available for model order estimation. Here, we consider the generalized Akaike information criterion (GAIC) due to its simplicity [38]. Specifically, the GAIC combines the negative logarithmic likelihood function with a penalty term proportional to the model order:

$$\begin{aligned} H_0: \hat{P}_{mn:0} = \arg\min_{P_{mn:0}} \big[&(K - P_{mn:0}) \ln\left(\tilde{\mathbf{x}}_{mn}^{H} \mathbf{P}_{\mathbf{Y}_{mn}}^{\perp} \tilde{\mathbf{x}}_{mn}\right) \\ &+ \beta(2P_{mn:0} + 1)\big], \end{aligned} \tag{55}$$

$$\begin{aligned} H_1: \hat{P}_{mn:1} = \arg\min_{P_{mn:1}} \Big[&(K - P_{mn:1}) \\ &\times \ln\left(\tilde{\mathbf{x}}_{mn}^{H} \mathbf{P}_{[\mathbf{P}_{\psi_{mn}}^{\perp} \mathbf{Y}_{mn}]}^{\perp} \tilde{\mathbf{x}}_{mn}\right) + \beta\left(2P_{mn:1} + 2\right)\Big], \end{aligned} \tag{56}$$

where β is a user parameter and a suggested choice is $\beta = 4\ln(\ln K)$ for one-dimensional complex data sequence in [38]. It is clear that model order estimation from (55)-(56) is affected by the fitting error and computation complexity caused by over-large estimates of model orders.

Once we have model order estimates, the test statistic of the parametric GLRT is given by the ratio of likelihood functions

This article has been accepted for publication in a future issue of this journal, but has not been fully edited. Content may change prior to final publication. Citation information: DOI 10.1109/JSTSP.2015.2467355, IEEE Journal of Selected Topics in Signal Processing

(48) and (49):

$$T_{\text{P-GLRT}} = \prod_{mn} \frac{\left(\tilde{\mathbf{x}}_{mn}^{\text{H}} \hat{\mathbf{P}}_{\mathbf{Y}_{mn}}^{\perp} \tilde{\mathbf{x}}_{mn}\right)^{K-\hat{P}_{mn:0}}}{\left(\tilde{\mathbf{x}}_{mn}^{H} \hat{\mathbf{P}}_{\left[\mathbf{P}_{\psi_{mn}}^{\perp} \mathbf{Y}_{mn}\right]}^{\perp} \tilde{\mathbf{x}}_{mn}\right)^{K-\hat{P}_{mn:1}}} \tag{57}$$

where $\hat{\mathbf{P}}_{\mathbf{Y}_{mn}}^{\perp}$ and $\hat{\mathbf{P}}_{\left[\mathbf{P}_{\psi_{mn}}^{\perp} \mathbf{Y}_{mn}\right]}^{\perp}$ are given by (51)-(52), respectively, by using the model order estimate obtained from (55)-(56). The proposed parametric MIMO detector is summarized in Algorithm 2.

- **Step A:** H_1 estimation
  1) Calculate $\hat{P}_{mn:1}$ from (56) for $m = 1, \ldots, M$ and $n = 1, \ldots, N$.
  2) Use $\hat{P}_{mn:1}$ to form the $(K - \hat{P}_{mn:1}) \times 1$ observational data $\tilde{\mathbf{x}}_{mn}$, and the projection matrix $\hat{\mathbf{P}}_{\left[\mathbf{P}_{\psi_{mn}}^{\perp} \mathbf{Y}_{mn}\right]}^{\perp}$ according to (52).
- **Step B:** H_0 estimation
  1) Calculate $\hat{P}_{mn:0}$ from (55) for $m = 1, \ldots, M$ and $n = 1, \ldots, N$.
  2) Use $\hat{P}_{mn:0}$ to form the $(K - \hat{P}_{mn:0}) \times 1$ observational data $\tilde{\mathbf{x}}_{mn}$, and the projection matrix $\hat{\mathbf{P}}_{\mathbf{Y}_{mn}}^{\perp}$ according to (51).
- **Step C:** Compute the test statistic from (57).

Algorithm 2: The proposed parametric detector.

It is worth noting that both the proposed sparsity based and the parametric MIMO detectors in (43) and (57) require no range training signals. Hence, they are immune to the range/location-dependent clutter problem suffered by conventional detectors which rely on range training. Furthermore, they also do not require a priori knowledge of disturbance structure (i.e., sparsity or model orders), which implies that both proposed detectors are fully adaptive and all the unknown parameters which describe the clutter characteristics are estimated from the test signal. Finally, by using the the asymptotic result for GLRT (see [23, p. 205] and also [15, Section III.D], it is easy to show that the test variables for both S-GLRT and P-GLRT are asymptotically central Chi-square distributed with $2MN$ degrees of freedom under H_0. Hence, both detectors achieve asymptotically constant false alarm rate (CFAR).

C. Target Velocity Estimation

In previous discussions of both the proposed S-GLRT and P-GLRT detectors, the target velocity parameters $\{v, \delta\}$ are assumed known. We consider herein the case when the target velocity is unknown and discuss how to estimate the associated parameters for both detectors.

1) Velocity Estimation for the S-GLRT: By substituting the estimates in (27), (28) and (31) into the likelihood function (25), it is easy to show that the target velocity parameters $\{v, \delta\}$ can be estimated by

$$\{\hat{v}, \hat{\delta}\} = \arg \min_{\{v,\delta\}} \prod_{mn} \left\| \mathbf{P}_{mn}^{\perp} (\mathbf{x}_{mn} - \hat{\mathbf{H}}_{mn} \hat{\boldsymbol{\gamma}}_{mn}) \right\|^2, \tag{58}$$

where $\mathbf{P}_{mn}^{\perp}$ is defined in (29), which depends on the steering vector $\mathbf{s}_{mn}(v, \delta)$. Note that the clutter parameters estimates $\{\hat{\mathbf{H}}_{mn}, \hat{\boldsymbol{\gamma}}_{mn}\}$ in (31) depend on $\mathbf{s}_{mn}(v, \delta)$ and hence are functions of the target velocity parameters. As such, (58) involves a 2-D search on $\{v, \delta\}$.

2) Velocity Estimation for the P-GLRT: Following the likelihood function in (49), it is readily shown that the MLEs of target velocity parameters are given by

$$\{\hat{v}, \hat{\delta}\} = \arg \min_{\{v,\delta\}} \sum_{mn} (K - \hat{P}_{mn:1}) \ln(\tilde{\mathbf{x}}_{mn}^{H} \mathbf{P}_{\left[\mathbf{P}_{\psi_{mn}}^{\perp} \mathbf{Y}_{mn}\right]}^{\perp} \tilde{\mathbf{x}}_{mn}) \tag{59}$$

where $\tilde{\mathbf{x}}_{mn}$, $\mathbf{Y}_{mn}$, $\mathbf{P}_{\psi_{mn}}^{\perp}$ and $\hat{P}_{mn:1}$ are defined in (50), (53), (54), and (56), respectively. Note that $\mathbf{P}_{\psi_{mn}}^{\perp}$ is a function of the target Doppler frequency observed by the (m, n)-th TX-RX pair and hence depends on the target velocity parameters $\{v, \delta\}$. Therefore, (59) also involves a 2-D search.

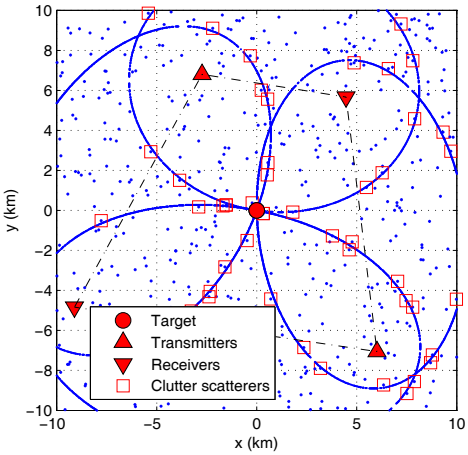

Fig. 3. A 2×2 multistatic radar scene.

TABLE I
LOCATION AND MOVING PARAMETERS OF THE TARGET AND SENSOR PLATFORMS

	speed (m/s)	moving angle (°)	locations (km)
Target	30	randomly chosen	(0, 0)
TX-1	250	65	(-2.85, 6.68)
TX-2	150	257	(6.03, -6.98)
RX-1	250	35	(4.65, 5.78)
RX-2	150	49	(-8.98, -4.93)

V. Simulation Results

In this section, we demonstrate the performance of the proposed sparsity based GLRT (S-GLRT) and fully adaptive parametric GLRT (P-GLRT) which are compared with several existing detectors through computer simulations. The distributed MIMO radar system consists of $M = N = 2$ TX and RX antennas covering a radar scene of 20 km $\times$ 20 km, as shown in Fig. 3. The position/moving parameters

This article has been accepted for publication in a future issue of this journal, but has not been fully edited. Content may change prior to final publication. Citation information: DOI 10.1109/JSTSP.2015.2467355, IEEE Journal of Selected Topics in Signal Processing

of the radar platforms and target are shown in Table I. For simplicity, the radar and the target are assumed to be located on a 2-dimensional plane. This allows Doppler effects of the target/clutter and location/motion induced clutter non-homogeneity and target Doppler to be adequately simulated without getting into a full-blown, high-fidelity 3-dimensional simulation, which is time consuming and beyond the scope of the current effort. As indicated in Table I, the target moves in a random direction which changes from one simulation to another, so that the average detection performance of the detectors can be obtained and used for comparison.

The moving target is located at the center of the radar scene. The target, along with the 2×2 TXs/RXs, specify four isoranges (ellipses) that, as shown in Fig. 3, intercept at the target location. Each isorange corresponds to one TX/RX pair. For clutter simulation, 500 clutter scatterers randomly distributed within the area are generated, and those which are located on any of the isoranges contribute to the clutter associated with that TX/RX pair as in (10). To determine if, say, the i-th clutter scatterer is located on the (m,n)-th isorange, we compare the bistatic range R_{mn} of the target associated with the (m,n)-th isorange and the bistatic range R_{mn}^i of the clutter scatterer [39]

$$|R_{mn}^i - R_{mn}| \leq \frac{c}{2B}, \tag{60}$$

where c denotes the speed of light and B the bandwidth of the radar. In our simulation, we have $B = 3$ MHz, the carrier frequency $f_c = 1$ GHz, the pulse repetition frequency (PRF) $= 4000$ Hz, and the number of pulses $K = 128$. This leads to clutter ranks $L_{mn} = \{12, 13, 11, 14\}$ with the Doppler frequencies shown in Table II. It is seen that due to platform motion, the clutter Doppler frequencies are spread over the entire Doppler bandwidth.

TABLE II
CLUTTER DOPPLER FREQUENCIES

TX1-RX1(Hz)	TX1-RX2(Hz)	TX2-RX1(Hz)	TX2-RX2(Hz)
1389	144	-1287	-330
-762	347	-1007	-27
-1169	333	654	-24
-1438	-808	497	-811
1281	-792	301	-26
-1177	96	1301	54
-1093	-804	-274	-806
-1615	355	1319	-439
1326	341	-598	76
-1229	284	-834	-182
1362	-1306	826	-19
-1630	-1333		-58
	193		-486
			-768

A. Detection Performance

We consider the proposed S-GLRT (43), P-GLRT (57), the SCM detector (17) and the robust SCM detector (18). For all these detectors, we consider two cases involving the target velocity (speed and direction) which is assumed known and, respectively, unknown. The latter case is to examine the effect of target velocity estimation on detection performance, in correspondence with the discussion in Section IV-C. For both cases, $\bar{\mathbf{H}}$ is a 128×256 over-complete Fourier dictionary for the S-GLRT usage.

First, we consider a *non-fluctuating* target model where the target amplitudes α_{mn} are assumed fixed from trial to trial. The clutter coefficients $\gamma_{mn,i}$ [cf. (12)] are compound-Gaussian that is K-distributed clutter with a scaling factor of 5 and a shape factor of 0.2. The signal-to-clutter-plus-noise ratio (SCNR) is defined as

$$\text{SCNR} = \sum_{m=1}^{M}\sum_{n=1}^{N} |\alpha_{mn}|^2 \mathbf{s}_{mn}^{\text{H}} \mathbf{R}_{mn}^{-1} \mathbf{s}_{mn}, \tag{61}$$

while the clutter-to-noise ratio (CNR) is defined as

$$\text{CNR} = \frac{\sum\limits_{m,n} \text{tr}\{\mathbf{R}_{\text{c},mn}\}}{KMN\sigma_{mn}^2}. \tag{62}$$

The target moving direction is randomly chosen according to a uniform distribution over the range $[0^\circ, 360^\circ]$ in every simulation trial.

The receiver operation characteristics (ROC) curves of the detectors are shown in Fig. 4(a) for the known target velocity case and Fig. 4(b) for the unknown target velocity case. As a benchmark, the clairvoyant MF detector (15) is also included in the comparison. The proposed detectors do not use any training, but for the SCM and the robust SCM detectors, $T = 144$ training signals are used to estimate each covariance matrix $\mathbf{R}_{mn}$ and the total training size is $4 \times 144 = 576$. The results in Fig. 4 show that the proposed detectors significantly outperform the covariance matrix based detectors. Comparisons between Fig. 4(a) and Fig. 4(b) reveal that all considered detectors experience some loss in detection performance when the target velocity is unknown.

Fig. 6 shows the detection performance of proposed and other detectors under different SCNR, assuming unknown target velocity and non-fluctuating target amplitude. Both the S-GLRT and P-GLRT detectors do not use any training data and outperform the SCM-based detectors which use $T = 144$ training data, and the advantage is more significant at higher SCNR.

Next, we consider a *fluctuating* target model where the target amplitudes α_{mn} are changing from one trial to another, following a complex Gaussian distribution with zero mean and variance $\sigma_{\alpha_{mn}}^2 = 1$ for each TX-RX pair. In this case, the SCNR is defined as

$$\text{SCNR} = \sum_{m=1}^{M}\sum_{n=1}^{N} \sigma_{\alpha,mn}^2 \mathbf{s}_{mn}^{\text{H}} \mathbf{R}_{mn}^{-1} \mathbf{s}_{mn}. \tag{63}$$

Fig. 5 plots the performance curves of the proposed, MF, SCM, and robust SCM detectors, where all simulation parameters except α_{mn} are the same as those in Fig. 4. It is also shown that the proposed detectors have better performance than the covariance matrix based detectors.

B. Model Order Selection

To illustrate the effect of model order selection on the proposed P-GLRT detector, Fig. 7 depicts the detection performance of the detector when it is used with several different

This article has been accepted for publication in a future issue of this journal, but has not been fully edited. Content may change prior to final publication. Citation information: DOI 10.1109/JSTSP.2015.2467355, IEEE Journal of Selected Topics in Signal Processing

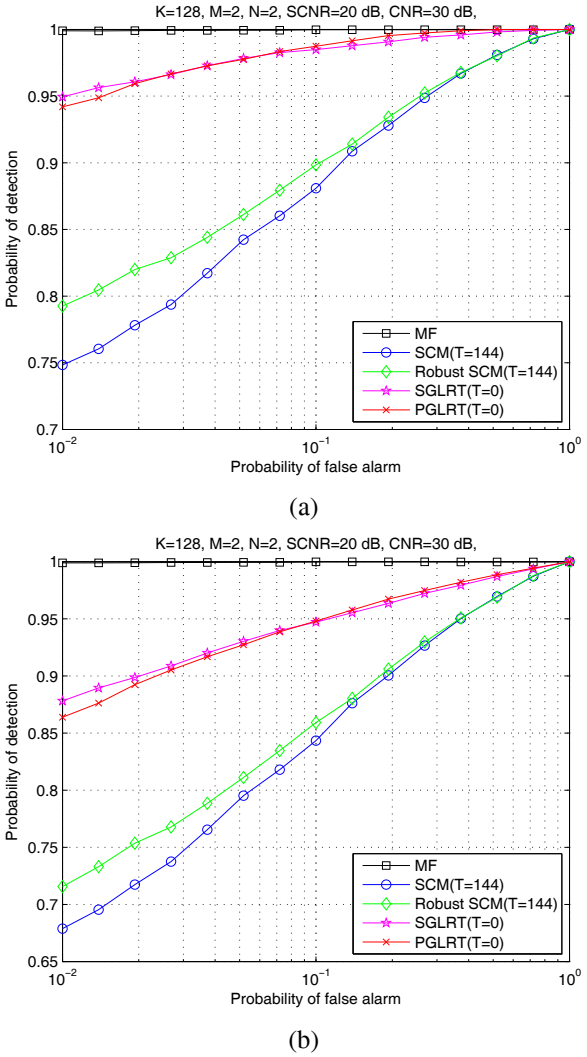

Fig. 4. ROC curves with non-fluctuating target amplitudes in the compound-Gaussian clutter: (a) known target velocity; (b) unknown target velocity.

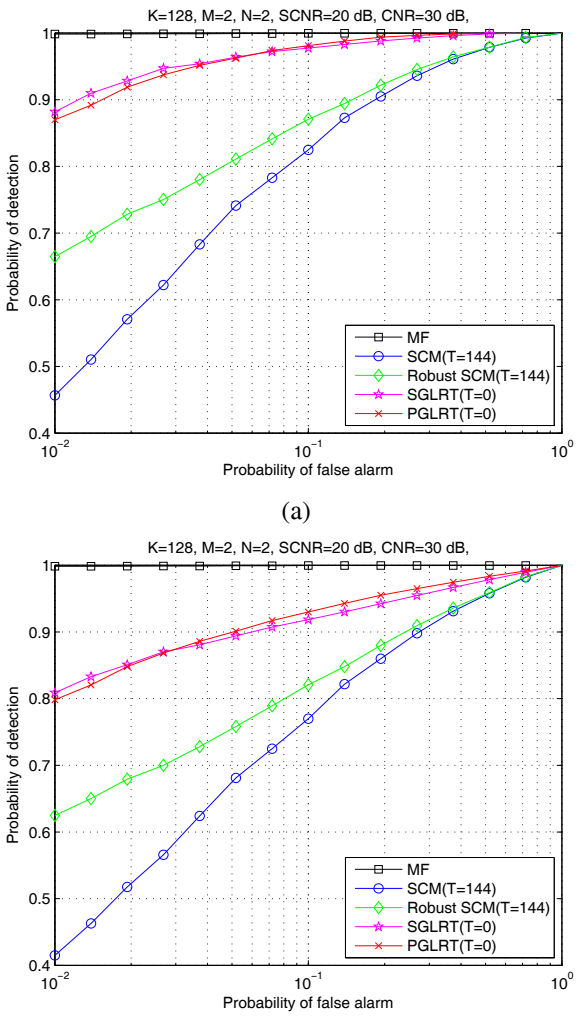

Fig. 5. ROC curves with fluctuating target amplitudes in the compound-Gaussian clutter: (a) known target velocity; (b) unknown target velocity.

sets of model orders, including the one obtained by using our proposed model order selection method. It is noted that the set $\{12, 13, 11, 14\}$ are identical to the true clutter ranks as discussed earlier and hence treated as the "true" model order. On the other hand, the model order set $\{4, 4, 4, 4\}$ corresponds to the case when the orders are underestimated, while $\{20, 20, 20, 20\}$ is the case when the orders are overestimated. It can be seen that the proposed fully adaptive P-GLRT which uses the estimated model orders offers detection performance close to that using the true orders. In addition, the usage of the over-/under-estimated model orders in the P-GLRT results in significant performance losses.

VI. Conclusions

In this paper, we examined the moving target detection (MTD) problem in distributed MIMO radar with sensors on moving platforms. A major issue is to deal with the bistatic geometry induced, location dependent clutter non-homogeneity, which is further worsened by platform motion. We examined the effects of platform motion on the target/clutter responses

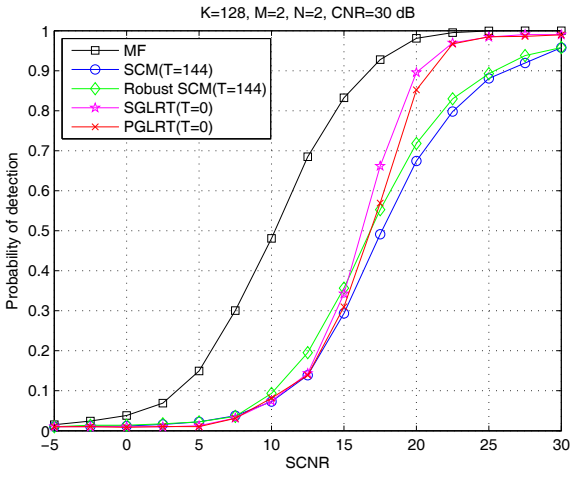

Fig. 6. Probability of detection versus SCNR with non-fluctuating target amplitudes and unknown target velocity.

This article has been accepted for publication in a future issue of this journal, but has not been fully edited. Content may change prior to final publication. Citation information: DOI 10.1109/JSTSP.2015.2467355, IEEE Journal of Selected Topics in Signal Processing

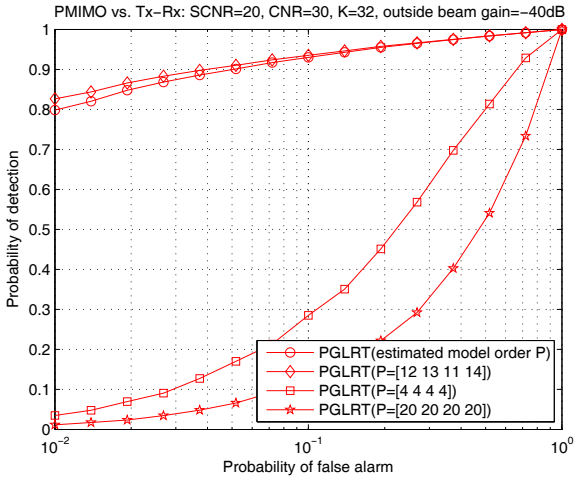

Fig. 7. ROC curves for the proposed P-GLRT with different sets of AR model orders.

and, based on our analysis, developed two new detectors by exploiting suitable sparsity based and, respectively, a parametric autoregressive (AR) based clutter model. Both detectors were developed within the GLRT framework and do not require training signals. Numerical results show that the proposed detector offer notable improvement over the conventional covariance matrix based detectors in non-homogeneous clutter environments. The two proposed detectors are similar to each other in general. There is no clear picture when one performs better than the other, and their relation is subject to further investigation.

REFERENCES

[1] M. C. Wicks, "Radar the next generation-sensors as robots," in *Proceedings of the International Conference on Radar*, September 2003, pp. 8–14.

[2] W. M. DeBusk, "Unmanned aerial vehicle systems for disaster relief: Tornado alley," in *AIAA Infotech@Aerospace Conference*, vol. AIAA-2010-3506, Atlanta, GA, April 2010.

[3] A. K. Mitra, "Position-adaptive UAV radar for urban environments," in *Proceedings of the International Radar Conference*, September 2003, pp. 303–308.

[4] C. E. Schwartz, T. G. Bryant, J. H. Cosgrove, G. B. Morse, and J. K. Noonan, "A radar for unmanned air vehicles," *The Lincoln Laboratory Journal*, vol. 3, no. 1, pp. 119–143, 1990.

[5] R. L. Moses, L. C. Potter, and M. Cetin, "Wide angle SAR imaging," in *Proc. SPIE*, vol. 5427, April 2004, pp. 164–175.

[6] M. Weiß, O. Peters, and J. Ender, "First flight trials with ARTINO," in *Proceedings of the 7th Conference on European Synthetic Aperture Radar (EUSAR)*, Friedrichshafen, Germany, June 2008, pp. 1–4.

[7] A. De Maio and M. Lops, "Design principles of MIMO radar detectors," *IEEE Transactions on Aerospace and Electronic Systems*, vol. 43, no. 3, pp. 886–898, July 2007.

[8] J. Li and P. Stoica, "MIMO radar with colocated antennas," *IEEE Signal Processing Magazine*, vol. 24, no. 5, pp. 106–114, September 2007.

[9] N. A. Goodman, "Optimum and decentralized detection for multistatic airborne radar," *IEEE Transactions on Aerospace and Electronic Systems*, vol. 43, no. 2, pp. 806–813, April 2007.

[10] A. M. Haimovich, R. S. Blum, and L. J. Cimini, "MIMO radar with widely separated antennas," *IEEE Signal Processing Magazine*, vol. 25, no. 1, pp. 116–129, January 2008.

[11] Q. He, N. H. Lehmann, R. S. Blum, and A. M. Haimovich, "MIMO radar moving target detection in homogeneous clutter," *IEEE Transactions on Aerospace and Electronic Systems*, vol. 46, no. 3, pp. 1290–1301, July 2010.

[12] C. Y. Chong, F. Pascal, J. P. Overlez, and M. Lesturgie, "Adaptive MIMO radar detection in non-Gaussian and heterogeneous clutter considering fluctuating targets," in *Proceedings of the IEEE Workshop on Statistical Signal Processing (SSP 09)*, Cardiff, Wales, UK, September 2009.

[13] C. Y. Chong, F. Pascal, J.-P. Ovarlez, and M. Lesturgie, "MIMO radar detection in non-Gaussian and heterogeneous clutter," *IEEE Journal of Selected Topics in Signal Processing*, vol. 4, no. 1, pp. 115–126, February 2010.

[14] P. Wang, H. Li, and B. Himed, "Moving target detection using distributed MIMO radar in clutter with nonhomogeneous power," *IEEE Transactions on Signal Processing*, vol. 59, no. 10, pp. 4809–4820, Oct. 2011.

[15] ——, "A parametric moving target detector for distributed MIMO radar in non-homogeneous environment." *IEEE Transactions on Signal Processing*, vol. 61, no. 9, pp. 2282–2294, May 2013.

[16] J. Liu, Z.-J. Zhang, Y. Cao, and S. Yang, "A closed-form expression for false alarm rate of adaptive MIMO-GLRT detector with distributed MIMO radar," *Signal Processing*, no. 9, pp. 2771–2776, September 2013.

[17] N. J. Willis, *Bistatic Radar*, 2nd ed. SciTech Publishing, 2005.

[18] J. Ward, "Space-time adaptive processing for airborne radar," Lincoln Laboratory, MIT, Technical Report 1015, December 1994.

[19] M. A. Richards, *Fundamentals of Radar Signal Processing*. McGraw-Hill, 2005.

[20] F. Gini and M. Greco, "Covariance matrix estimation for CFAR detection in correlated heavy tailed clutter," *IEEE Transactions on Signal Processing*, no. 12, pp. 1847–1859, December 2002.

[21] E. Conte, A. De Maio, and G. Ricci, "Recursive estimation of the covariance matrix of a compound-gaussian process and its application to adaptive CFAR detection," *IEEE Transactions on Signal Processing*, vol. 50, no. 8, pp. 1908–1915, August 2002.

[22] F. Pascal, Y. Chitour, P. Forster, and P. Larzabal, "Covariance structure maximum likelihood estimates in compound gaussian noise: existence and algorithm analysis," *IEEE Transactions on Signal Processing*, no. 1, pp. 34–48, January 2008.

[23] S. M. Kay, *Fundamentals of Statistical Signal Processing: Detection Theory*. Upper Saddle River, NJ: Prentice Hall, 1998.

[24] J. A. Tropp and A. C. Gilbert, "Signal recovery from random measurements via orthogonal matching pursuit," *IEEE Transactions on Information Theory*, no. 12, pp. 4655–4666, December 2007.

[25] S. Chen, D. Donoho, and M. Saunders, "Atomic decomposition by basis pursuit," *Society for Industrial and Applied Mathmatics Journal on Scientific Computing*, vol. 20, no. 1, pp. 33–61, 1998.

[26] S. Haykin, editor, *Array Signal Processing*. Englewood Cliffs, NJ: Prentice Hall, 1985.

[27] A. L. Swindlehurst and P. Stoica, "Maximum likelihood methods in radar array signal processing," *Proceedings of the IEEE*, vol. 86, pp. 421–441, February 1998.

[28] J. R. Román, M. Rangaswamy, D. W. Davis, Q. Zhang, B. Himed, and J. H. Michels, "Parametric adaptive matched filter for airborne radar applications," *IEEE Transactions on Aerospace and Electronic Systems*, vol. 36, no. 2, pp. 677–692, April 2000.

[29] G. Alfano, A. De Maio, and A. Farina, "Model-based adaptive detection of range-spread targets," *IEE Proc.-Radar Sonar Nacig.*, no. 1, pp. 2–10, February 2004.

[30] M. Greco, F. Bordoni, and F. Gini, "X-band sea-clutter nonstationarity: influence of long wave," *IEEE Journal of Oceanic Engineering*, no. 2, pp. 269–283, April 2004.

[31] K. J. Sohn, H. Li, and B. Himed, "Parametric Rao test for multichannel adaptive signal detection," *IEEE Transactions on Aerospace and Electronic Systems*, vol. 43, no. 3, pp. 920–933, July 2007.

[32] ——, "Parametric GLRT for multichannel adaptive signal detection," *IEEE Transactions on Signal Processing*, vol. 55, no. 11, pp. 5351–5360, November 2007.

[33] P. Wang, H. Li, , and B. Himed, "A new parametric GLRT for multichannel adaptive signal detection," *IEEE Transactions on Signal Processing*, vol. 58, no. 1, pp. 317–325, January 2010.

[34] ——, "A Bayesian parametric test for multichannel adaptive signal detection in nonhomogeneous environments," *IEEE Signal Processing Letters*, vol. 17, no. 4, pp. 351–354, April 2010.

[35] ——, "Knowledge-aided parametric tests for multichannel adaptive signal detection," *IEEE Transactions on Signal Processing*, vol. 59, no. 12, pp. 5970–5982, Dec. 2011.

[36] C. Jiang, H. Li, and M. Rangaswamy, "Conjugate gradient parametric detection of multichannel signals," *IEEE Transactions on Aerospace and Electronic Systems*, vol. 48, no. 2, pp. 1521–1536, April 2012.

This article has been accepted for publication in a future issue of this journal, but has not been fully edited. Content may change prior to final publication. Citation information: DOI 10.1109/JSTSP.2015.2467355, IEEE Journal of Selected Topics in Signal Processing

[37] P. Wang, Z. Wang, H. Li, and B. Himed, "Knowledge-aided parametric adaptive matched filter with automatic combining for covariance estimation," *IEEE Transactions on Signal Processing*, vol. 62, no. 18, pp. 4713–4722, Sep. 2014.

[38] T. Soderstrom and P. Stoica, *System Identification*. London: Prentice-Hall, 1989.

[39] K. J. Bell, J. T. Johnson, C. J. Baker, G. E. Smith, and M. Rangaswamy, "Modeling and simulation for multistatic coherent MIMO radar," in *Proceedings of the 2013 IEEE Radar Conference*, April 2013, pp. 1–6.

PLACE PHOTO HERE

Hongbin Li (M'99-SM'08) received the B.S. and M.S. degrees from the University of Electronic Science and Technology of China, in 1991 and 1994, respectively, and the Ph.D. degree from the University of Florida, Gainesville, FL, in 1999, all in electrical engineering.

From July 1996 to May 1999, he was a Research Assistant in the Department of Electrical and Computer Engineering at the University of Florida. Since July 1999, he has been with the Department of Electrical and Computer Engineering, Stevens Institute of Technology, Hoboken, NJ, where he became a Professor in 2010. He was a Summer Visiting Faculty Member at the Air Force Research Laboratory in the summers of 2003, 2004 and 2009. His general research interests include statistical signal processing, wireless communications, and radars.

Dr. Li received the IEEE Jack Neubauer Memorial Award in 2013 from the IEEE Vehicular Technology Soceity, the Outstanding Paper Award from the IEEE AFICON Conference in 2011, the Harvey N. Davis Teaching Award in 2003 and the Jess H. Davis Memorial Award for excellence in research in 2001 from Stevens Institute of Technology, and the Sigma Xi Graduate Research Award from the University of Florida in 1999. He has been a member of the IEEE SPS Signal Processing Theory and Methods Technical Committee (TC) and the IEEE SPS Sensor Array and Multichannel TC, an Associate Editor for *Signal Processing* (Elsevier), *IEEE Transactions on Signal Processing*, *IEEE Signal Processing Letters*, and *IEEE Transactions on Wireless Communications*, as well as a Guest Editor for *IEEE Journal of Selected Topics in Signal Processing* and *EURASIP Journal on Applied Signal Processing*. He has been involved in various conference organization activities, including serving as a General Co-Chair for the 7th IEEE Sensor Array and Multichannel Signal Processing (SAM) Workshop, Hoboken, NJ, June 17-20, 2012. Dr. Li is a member of Tau Beta Pi and Phi Kappa Phi.

PLACE PHOTO HERE

Zhe Wang (S'12) received the B.S. degree in 2008 and M.S. degree in 2010 from the Dalian University of Technology (DLUT), Dalian, all in electrical engineering. He is currently pursuing the Ph.D degree in electrical engineering at the Stevens Institute of Technology, Hoboken, NJ.

Since 2012 he has been a Research Assistant in the Department of Electrical and Computer Engineering at Stevens. His current research interests are in MIMO radar, digital signal processing, multichannel signal processing, adaptive detection and parameter estimation, and sparse signal processing.

PLACE PHOTO HERE

Jun Liu (S'11-M'13) received the B.S. degree in mathematics from Wuhan University of Technology, China, in 2006, the M.S. degree in mathematics from Chinese Academy of Sciences, China, in 2009, and the Ph.D. degree in electrical engineering from Xidian University, China, in 2012.

From July 2012 to December 2012, he was a Post-doctoral Research Associate in the Department of Electrical and Computer Engineering, Duke University, Durham, NC, USA. From January 2013 to September 2014, he was a Post-doctoral Research Associate in the Department of Electrical and Computer Engineering, Stevens Institute of Technology, Hoboken, NJ, USA. He is now with the National Laboratory of Radar Signal Processing, Xidian University, where he is an Associate Professor. His research interests include statistical signal processing, optimization algorithms, passive sensing, and multistatic radar.

PLACE PHOTO HERE

Braham Himed received his Engineer Degree in electrical engineering from Ecole Nationale Polytechnique of Algiers in 1984, and his M.S. and Ph.D. degrees both in electrical engineering, from Syracuse University, Syracuse, NY, in 1987 and 1990, respectively. Dr. Himed is a Technical Advisor with the Air Force Research Laboratory, Sensors Directorate, RF Technology Branch, in Dayton Ohio, where he is involved with several aspects of radar developments. His research interests include detection, estimation, multichannel adaptive signal processing, time series analyses, array processing, adaptive processing, waveform diversity, MIMO, passive radar, and over the horizon radar. Dr. Himed is the recipient of the 2001 IEEE region I award for his work on bistatic radar systems, algorithm development, and phenomenology. He is a Fellow of the IEEE and the Vice-Chair of the AES Radar Systems Panel. He is the recipient of the 2012 IEEE Warren White award for excellence in radar engineering. Dr. Himed is also a Fellow of AFRL (Class of 2013).